Aerodynamic Design of Axial Flow Turbine for a Small Gas Turbine Engine

D. Harish, R. D. Bharathan, Sharad Kapil, S. V. Ramana Murthy, and D. Kishore Prasad

Abstract Small gas turbines have been used in many unmanned aerial vehicle (UAV) applications. For UAV, the design of gas turbine engine is driven by its simplicity, cost-effectiveness and reliability, and moderate fuel efficiency. This paper describes the aerodynamic design and salient features of a single-stage axial turbine designed for powerplant of UAV application. Profile, secondary and tip clearance losses are dominant due to reduced blade heights, Reynolds number, and manufacturing constraints. The transonic axial turbine is designed with low-aspect ratio and moderate stage loading. The design point pressure ratio is 2.3, and the target efficiency is 86%.

Nomenclature

C	Chord (mm)
C_p	Specific heat at constant pressure (J/Kg-K)
R	Radius (mm)
S	Pitch (mm)
T_{max}	Maximum thickness of aerofoil (mm)
X	Axial distance from leading edge (mm)
ΔT	Total temperature drop across turbine (K)

D. Harish · R. D. Bharathan (✉) · S. Kapil · S. V. Ramana Murthy · D. Kishore Prasad
DRDO-Gas Turbine Research Estabilishment, Bengaluru, India
e-mail: bharathan.gtre@gov.in

D. Harish
e-mail: harishd.gtre@gov.in

S. Kapil
e-mail: sharadkapil.gtre@gov.in

S. V. Ramana Murthy
e-mail: ramanamurthy.gtre@gov.in

D. Kishore Prasad
e-mail: kishoreprasadd.gtre@gov.in

G. Sivaramakrishna et al. (eds.), *Proceedings of the National Aerospace Propulsion Conference*, Lecture Notes in Mechanical Engineering,
https://doi.org/10.1007/978-981-19-2378-4_6

k	Turbulence kinetic energy
ω	Turbulent frequency
η	Efficiency

Subscripts

m	Mean section
h	Hub section
t	Tip section

1 Introduction

In last few decades, small gas turbine engine (SGTE) has been increasingly used as powerplant for UAV application. Specific fuel consumption (SFC) is not of prime importance for this application as its operational time is limited. The following requirements are proposed to be met during developmental phase as proposed by Barbeau [1], Kidd [2], and Rideau [3]:

- Simplicity in design and robustness reduced part count to enhance reliability.
- High specific thrust for compactness.
- Low manufacturing cost.
- Long-term storage and no maintenance.

This paper describes the aerodynamic design of single-stage axial flow turbine for SGTE. A single-stage turbine is designed for the target efficiency of 86% with a pressure ratio of 2.3 such that all the above requirements are considered at preliminary design stage.

The drivers of this design are aerodynamic performance, producibility, low cost, and high reliability. These are achieved by incorporating manufacturing constraints at design phase, reducing weight, part count, and using integrated castings as much as possible. The component shall be designed to guarantee performance requirement.

2 Mean-line Design

The design point is chosen from several operating conditions based on higher rotational speed, turbine entry temperature, and pressure. Turbine stage is designed for nondimensional parameters shown in Table 1, which is obtained from thermodynamic cycle of SGTE. Once the spool speed is agreed upon between compressor and turbine designers, stage loading, flow coefficient, and mean reaction are selected to meet

Table 1 Turbine stage thermodynamic quasi nondimensional parameters

S. No.	Parameters	Units	Values
1	Mass flow function	kg$\sqrt{}$K/kPa	0.31
2	Specific work function	J/kg-K	186
3	Speed function	(rev/min)/$\sqrt{}$K	1172.0
4	Pressure ratio	–	2.3
5	Efficiency	%	86

the required aerodynamic performance, dimensional, and weight constraints. The selected parameters are shown in Table 2. Smith [4] proposed correlations between stage loading, flow coefficient, and efficiency of turbines with 0.5 mean reaction based on experimental results. These correlations serve as a qualitative tool to estimate the performance of the turbine stage during preliminary design phase. Figure 1 shows the Smith chart plotted based on the correlations indicating the chosen value of stage loading and flow coefficient.

Mean-line calculation is performed using in-house code based on Horlock [5], Denton [6] and modified based on Ramana Murthy et al. [7, 8]. Loss models, correlations for choice of chord and stagger and blade spacing as mentioned in Kacker and Okapuu [9] are incorporated in the in-house code.

Table 2 Turbine stage overall parameters

S. No.	Parameters	Values
1	Stage loading	1.43
2	Flow coefficient	0.53
3	Mean section reaction	0.45

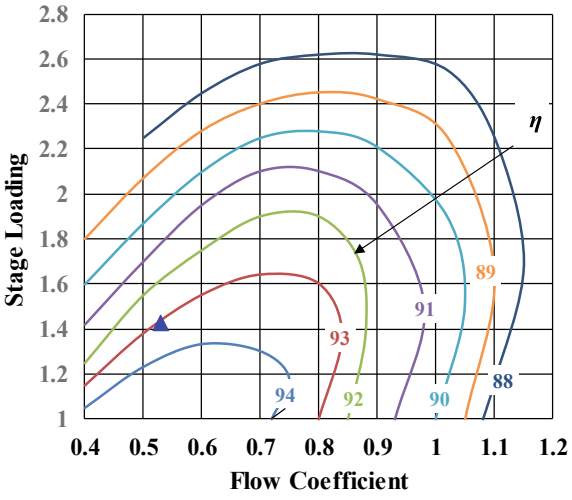

Fig. 1 Smith chart

3 Flowpath Design

Flowpath geometry, mean-line velocity triangle, number of blades are obtained from mean-line analysis. During this phase, multiple design iterations were carried out by adjusting the parameters to obtain cylindrical endwalls especially for the rotor which allow for constant tip clearance to be maintained and allow for easier inspection. The hub-endwall of the stator is suitably profiled to interface with the upstream combustor. Figure 2 shows the mean velocity triangle. Low mean reaction might lead to negative reaction at hub section (where gases may undergo compression instead of expansion). Hence, mean reaction of 0.45 is chosen.

Profile loss is minimized by choosing an optimal value of S/C and from this, the number of stators and blades can be determined. Zweifel coefficient is calculated from the velocity triangle, S/C and found to be in optimal range. The stagger angle is determined based on the flow angles between inlet and outlet from method proposed by Kacker and Okapuu [9]. Figure 3 shows the flowpath of the turbine stage.

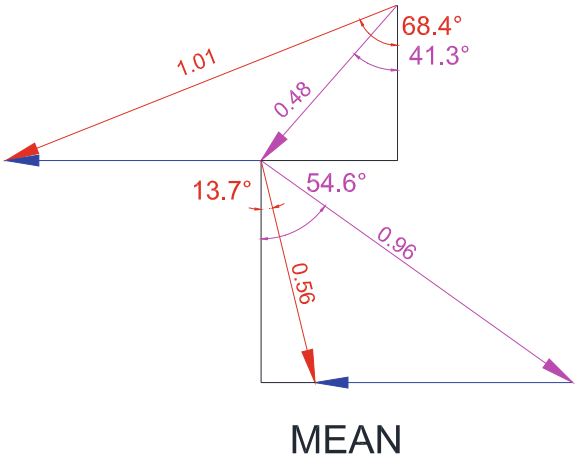

Fig. 2 Mean-line velocity triangle

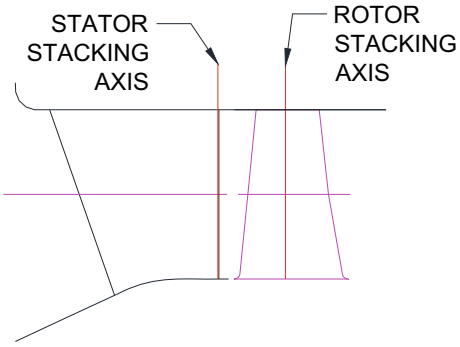

Fig. 3 Turbine stage flowpath

4 Hub-to-Tip Design

In hub-to-tip design, velocity triangles at hub, mean, tip section are obtained. An in-house streamline curvature code based on Denton [10] that solves steady, inviscid, axi-symmetric flow and satisfies radial equilibrium is used. Secondary flows dominate the flow at the endwalls of the turbine stage. Yoon et al. [11] studied the effect of tip clearance leakage flows due to tip reaction. It was suggested that increase in tip reaction will leads to increase tip clearance losses. Therefore, a spanwise controlled vortex with parabolic work distribution with maximum work extraction near the mean and minimum work extraction near the endwalls is adopted. This will help to minimize the secondary losses as well as tip clearance losses. Other parameters such as stator exit Mach number and angle, rotor inlet, and exit Mach numbers and angles as obtained from hub-to-tip analysis are found to be within the limits of industry best practices.

5 Profile Generation

Aerofoil profiles are generated using eleven parameters method by Pritchard [12]. This method is modified by Ramana Murthy and Kishore Kumar [13] to incorporate Bezier curves for constructing pressure and suction side curves instead of polynomials. This provides the flexibility to change the T_{max}/C while ensuring slope continuity over the generated profile. Table 3 shows some of the salient parameters of the profiles that was generated at this stage.

After completion of each section profile generation, in-house 2-D inviscid blade-to-blade time marching solver formulated by Denton [10] is used to estimate the surface Mach number over the profiles for both design and off-design conditions.

5.1 Stator

In SGTE, TET is much less compared to that of modern military jet engine. Hence, simple convective cooling is sufficient for stators. The stators are hollow and forms flowpath with combustor. The stators are designed using constant *S/C* ratio at all radii and stacked at the trailing edge circle center. The exit angle is maintained constant. In terms of manufacturing constraints, trailing edge (TE) thickness plays an important

Table 3 Salient profile parameters

S. No.	Parameters	Stator	Rotor
2	S/C	0.69	0.64
3	T_{max}/C (%)	18	20
4	h/C	0.85	2.0
5	Rh/Rt	0.65	0.65

role. Thicker TE is easier to manufacture but it leads to increase the TE losses. TE thickness is chosen such that it is easy to manufacture and minimizes the losses. Weiss and Fottner [14] suggested that aft-loading of stator reduces the profile and secondary losses. Hence, stator was designed for aft-loading by adjusting the Bezier control points. Three sections for stator are generated at three radial heights. The profiles are stacked at the trailing edge circle center. Figure 4 shows mean section profile designed using the method described above, and Fig. 5 shows the surface Mach number distribution over stator—hub, mean, and tip profiles.

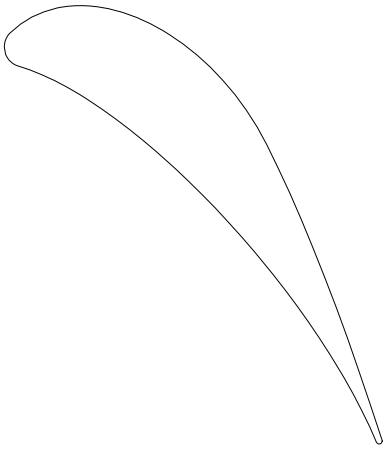

Fig. 4 Stator mean section

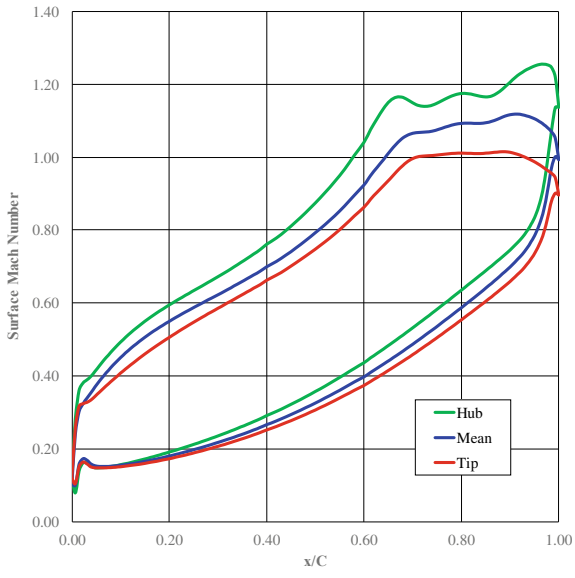

Fig. 5 Surface Mach number distribution over stator mean section

5.2 Rotor

Rotor blades are designed for an aspect ratio of two and stacked at the center of gravity of each section to eliminate bending stress. TE thickness is 20% higher as that of stator so that stresses at the TE of hub section is lower. Rotor blades metal temperature is always close to that of relative total temperature. During preliminary design, based on the estimated metal temperature, it is decided to design a solid blade without any cooling passage. Rotor blisk design was adopted as it significantly reduces weight and the number of components compared to conventional blade and disk design, thereby increasing reliability. The Bezier control points are adjusted such that the rotor sections are mid-loaded. Three sections for rotor blade were generated at three radial heights. The profiles are stacked over the centroid of each section to eliminate the bending stress due to centrifugal loads. Figure 6 shows the mean cross-section profile of rotor blade. Figure 7 shows the surface Mach number distribution over rotor—hub, mean, and tip profiles.

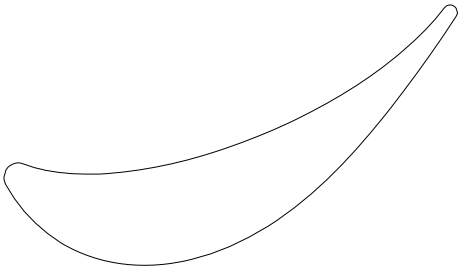

Fig. 6 Rotor mean section

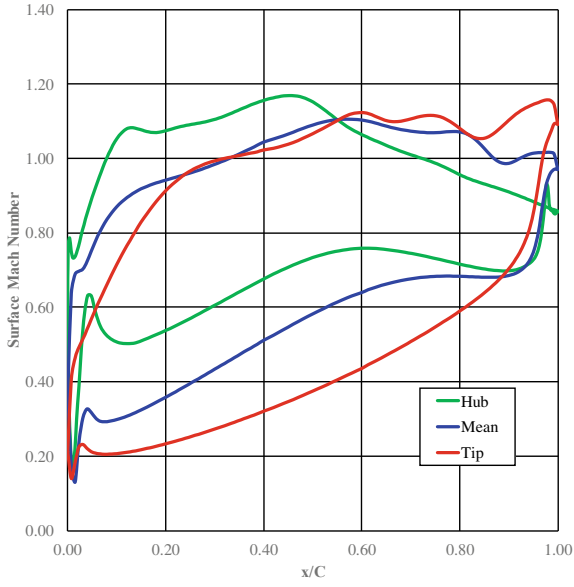

Fig. 7 Surface Mach number over rotor mean section

6 CFD Analysis

ANSYS CFX—commercial three-dimensional Navier–Stokes solver is used during the design phase. Reynolds averaged Navier–Stokes equation is discretized using finite volume method and solved for a steady state solution. Shear stress transport model is used for modeling the turbulence. In this *k*-epsilon, turbulence model is used in far field and *k*-ω turbulence model is used near the viscous regions, solutions are merged using blending function. A second order accurate skew upwind differencing scheme with physical advection correction is employed.

6.1 Grid Generation

The computational grid is generated using ANSYS CFX turbogrid. Automatic topology and meshing (ATM) method is used for stator and rotor blade. Sufficient grids are placed at the walls to capture the boundary layers. Grid independence was carried out. The skewness angle of the generated grid is kept between 35 and 155°, *y* plus less than 1, aspect ratio is kept below 100 and expansion ratio is below 1.2. Tip clearance value is set to be 1% of blade height, and it is modeled separately. The computational grid is shown in Fig. 8.

6.2 Boundary Condition

In stator domain, constant total pressure and radially varying total temperature based on the radial pattern factor are imposed at inlet. At inlet, 10% of blade height is used for eddy length scale and 10% is used for fractional intensity.

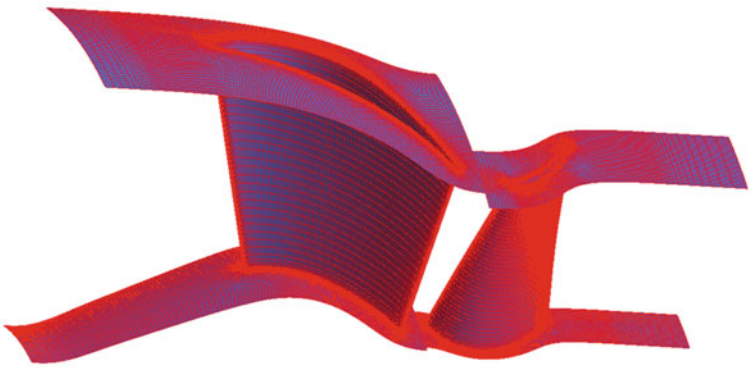

Fig. 8 Computational grid of turbine stage

At rotor domain, static pressure outlet is used. Mixing plane model is used between stator and rotor grid at the interface. Rotational periodicity along the axis of rotation is used at both stator and rotor.

Gas properties such as Cp, kinematic viscosity, thermal conductivity are calculated based on the fuel-to-air ratio and average temperature at inlet and exit plane.

7 Results and Discussion

The designed stage is analyzed using CFX and post-processed using CFX-post. Multiple CFD iterations were carried out to ensure the stage passed the required mass flow, and the blade angles were adjusted to minimize incidences and deviation. Figure 9 shows the blade-to-blade Mach number variation at midspan section. It can be observed that there is no sudden deceleration or flow separation bubble over the suction side of stator and rotor at midspan. The acceleration of the flow is smooth over the suction side on stator. The peak Mach number over the stator is higher compared to that of rotor because of reaction being 0.45. Iterations in CFD were carried out to avoid rotor blade leading edge local acceleration.

Figure 10 shows the surface streamline over stator suction side. Interaction of the secondary flow with the main flow is minimized as shown in Fig. 10. Figure 11 shows the streamline in the tip clearance region. The leakage flow over the tip clearance regions leads to formation of vortex structure which contributes to tip clearance losses.

The stator exit Mach number varies from 1.2 to 0.9 from hub-to-tip as seen from Fig. 12, corroborating the stator surface streamline pattern observed in Fig. 10.

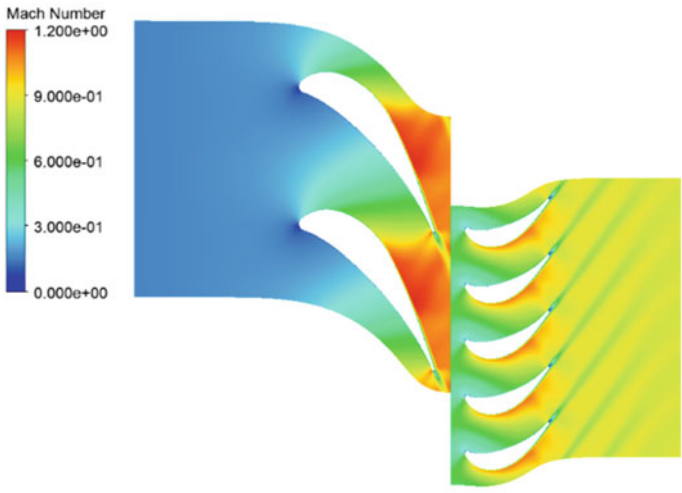

Fig. 9 Blade-to-blade Mach number distribution at midspan

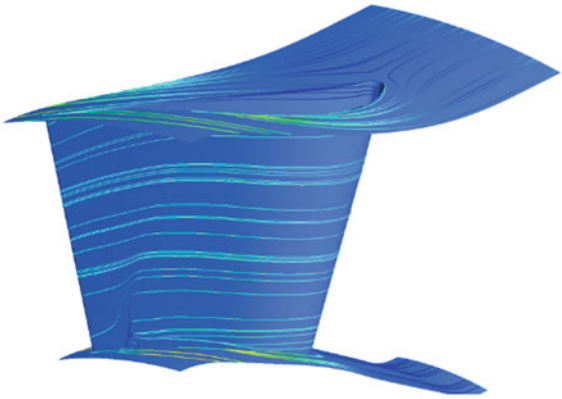

Fig. 10 Streamline over stator

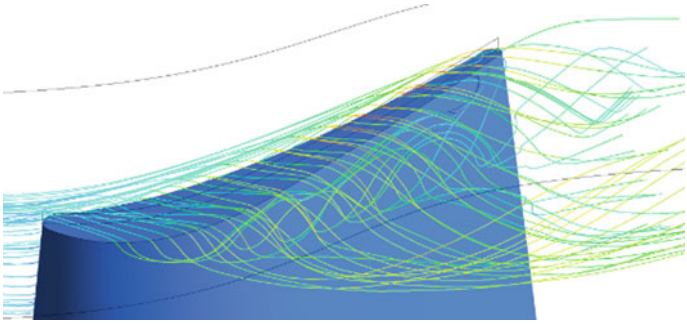

Fig. 11 Streamline in tip clearance region

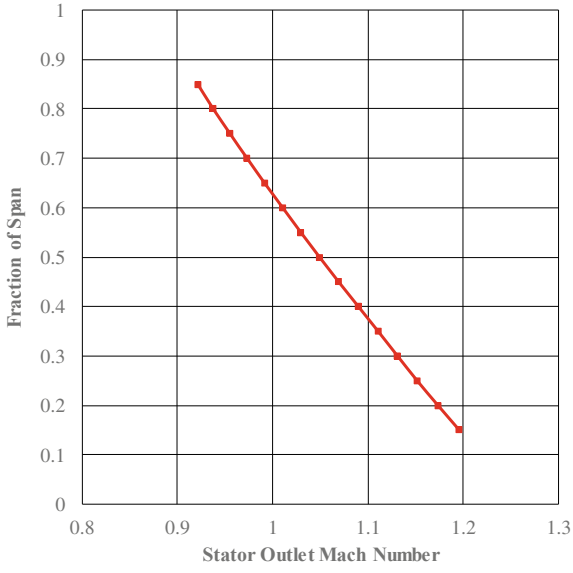

Fig. 12 Spanwise variation of stator outlet Mach number

Figures 13 and 14 show the rotor outlet relative flow angle and relative Mach number, respectively. The outlet angle varies within −45° and −55° degrees across the span, and the outlet relative Mach number varies from 0.7 to 0.95.

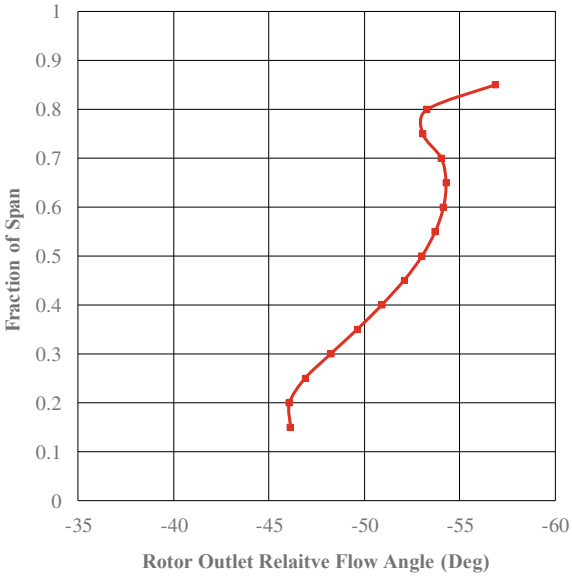

Fig. 13 Spanwise variation of rotor outlet relative flow angle

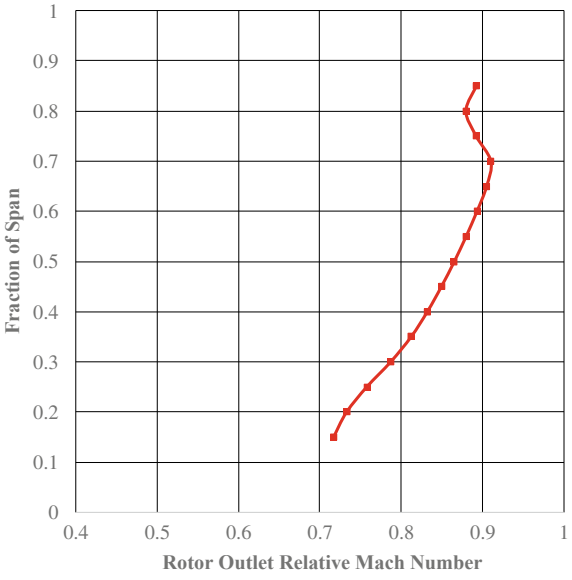

Fig. 14 Spanwise variation of rotor outlet relative Mach number

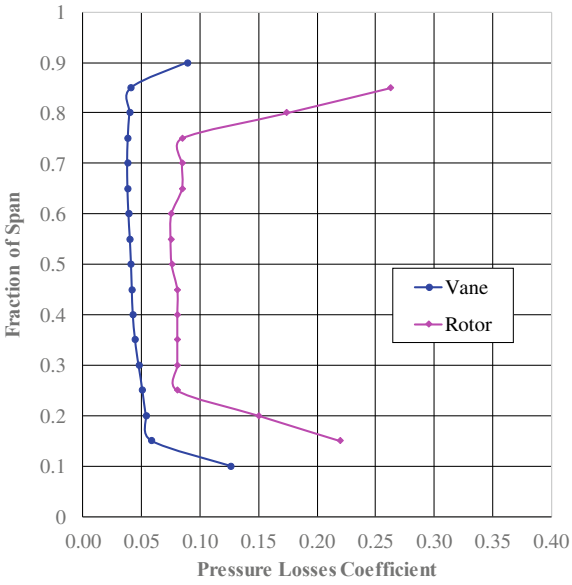

Fig. 15 Spanwise pressure loss coefficient of stator and rotor

Figure 15 shows the pressure loss coefficient variation for stator and rotor. For stator, losses increase near the endwall regions because of secondary flows. For rotor, secondary and tip leakage flows increase the losses near the endwall. During the preliminary design phase, parabolic work extraction is used and Fig. 16 shows

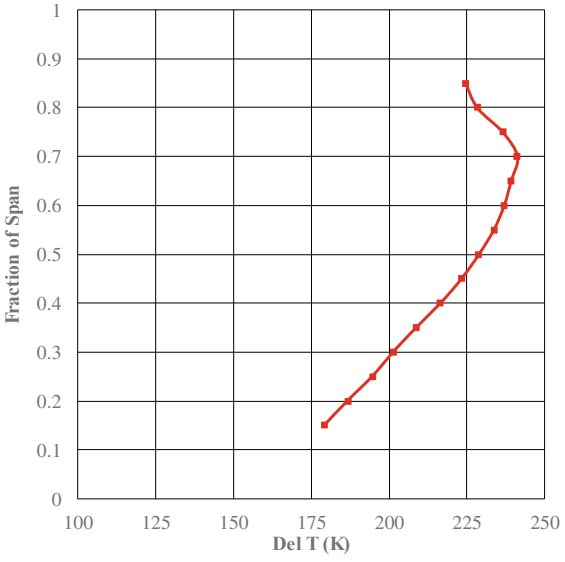

Fig. 16 Spanwise distribution of temperature drop

the total temperature drop across stage obtained from CFD results. And it can be seen that work extraction at the hub and tip are minimum as per design intent.

8 Conclusions

A single-stage transonic turbine is designed by considering all the constraints during design phase, and it meets the required performance parameters. The stage efficiency with tip clearance of 1% of blade height is estimated to 89% which is 3% higher than target efficiency.

Acknowledgements The authors thank Director, GTRE for giving permission to present this work.

References

1. Barbeau DE (1981) A family of small, low cost turbojet engines for short life applications. ASME paper 81-GT-205
2. Kidd WE (1973) Turbine powerplants for missiles—cost improvement requirements. SAE Transactions, pp 1250–1257
3. Rideau JF, Guyader G, Cloarec A (2008) MICROTURBO families of turbojet engine for missiles and Uav's from the TR60 to the new bypass turbojet engine generation. In: 44th AIAA/ASME/SAE/ASEE joint propulsion conference and exhibit, p 4590
4. Smith SF (1965) A simple correlation of turbine efficiency. J R Aeronaut Soc 69:467–470
5. Horlock JH (1966) Axial flow turbines. Butterworths
6. Denton JD (1972) A computer program for steam turbine performance prediction. ARC 34-229, Turbo 248
7. Ramana Murthy SV, Ganesh R, Krishnaiah TV (2007) Aerodynamic improvement of low pressure turbine using 3D viscous flow computation. ISABE
8. Murthy SR, Kumar SK (2012) Parametric study of axial flow turbine for mean-line design and blade elements. In: Gas turbine India conference, vol 45165. American Society of Mechanical Engineers, pp 131–137
9. Kacker SC, Okapuu U (1982) A mean line prediction method for axial flow turbine efficiency. ASME J Eng Power 104(1):111–119
10. Denton JD (1983) An improved time marching method for turbo machinery flow calculation. J Eng Power 105:514–524
11. Yoon S, Curtis E, Denton J, Longley J (2010) The effect of clearance on shrouded and unshrouded turbines at two levels of reaction. In: Proceedings of the ASME turbo expo 2010: power for land, sea, and air. Volume 7: turbomachinery, parts A, B, and C. Glasgow, UK, pp 1231–1241. ASME
12. Pritchard LJ (1985) An eleven parameter axial turbine airfoil geometry model. ASME paper 85-GT-219
13. Ramana Murthy SV, Kishore Kumar S (2014) Development and validation of a Bezier curve based profile generation method for axial flow turbines. IJSTR 3(12)
14. Weiss AP, Fottner L (1995) The influence of load distribution on secondary flow in straight turbine cascades. ASME J Turbomach 117(1):133–141